31st Annual International Conference of the IEEE EMBS
Minneapolis, Minnesota, USA, September 2-6, 2009

A passive microfluidic device for plasma extraction from whole human blood

E. Sollier, M. Cubizolles, M. Faivre, Y. Fouillet, and J. L. Achard

Abstract—**Promising microfluidic devices are proposed herein to continuously and passively extract plasma from whole human blood. These designs are based on the red cells lateral migration and the resulting cell-free layer locally expanded by geometric singularities, such as an abrupt enlargement of the channel or a cavity adjacent to the channel. After an explanation of flow patterns, devices are experimentally and biologically validated for plasma extraction. They are also successively optimized with extraction yields up to 17.8% for a 1:20 blood injected at 100µL/min.**

I. Introduction

HUMAN plasma proteins are representative of many complex patient pathologic states. Therefore plasma is the sample of choice in 90% of blood diagnosis tests. Separation of plasma from blood cells is most of the time performed by means of centrifugation. However, for the total integration of blood analysis in a chip, microfluidic plasma separation from blood cells is necessary. This step has rarely been successfully investigated and still remains a topical challenge [1].

Continuous flow separation can be achieved by many emerging techniques [1, 2, 3], based on passive hydrodynamics in microchannels [4] (such as cross flow filtration [5, 6]) or combining hydrodynamics with a force field (such as electric, magnetic, acoustic [7] or optic). Most attractive future solutions for continuous plasma extraction are passive migration devices that have the advantage to be faster and suitable for hardly diluted blood. They do not suffer from buffer incompatibilities and don't need filters nor complex fabrication technology [8, 9, 10, 11].

Herein innovating and promising devices are proposed to continuously extract plasma from whole human blood using only passive microfluidic effects. More precisely, the aim of our work is to strongly and locally enhance the well-known cell-free layer phenomena by geometric singularities, such as an abrupt enlargement of the channel or a cavity adjacent to the channel. Flow patterns are firstly explained. Then devices are proposed, experimentally optimized and finally biologically validated.

Manuscript received April 2, 2009. This work was supported by the CEA and more especially the Technologies for Health programs.

E. Sollier, M. Cubizolles, M. Faivre and Y. Fouillet are with the Department of Technology for Biology and Health, CEA-LETI-Minatec, 38054 Grenoble, France (corresponding author phone: 33-(0)4 38 78 28 02; fax: 33-(0)4 38 78 57 87; e-mail: elodie.sollier@cea.fr).

J. L. Achard is with the Laboratoire des Ecoulements Géophysiques et Industriels, Domaine Universitaire, 38041 Grenoble, France.

II. Experimental

A. Microfluidic chips fabrication

The microfluidic chips are made of polydimethylsiloxane (PDMS, Sylgard 184, Dow Corning) according to classical PDMS process: polymer solution mixing (ratio 5/1), pouring, degasing, curing (65°C, 1h), and surfaces activation (20W, 20sec, Plasma 0_2, OAST Products Inc) to seal the device. To do so, a microfabricated silicon mold is used, created by a conventional soft lithography process that allows the use of a fast prototyping for quick optimization designs.

B. Blood sample and injection

Tests are performed with human blood drawn from healthy volunteers, in EDTA tubes to avoid coagulation, and 1:20 diluted with phosphate buffered-saline (PBS) before injection.

Blood injections are observed under an optical microscope (Axioplan2, Zeiss) with photographs captured by a video camera (DP71, Olympus).

C. Plasma characterization

Extracted plasma is biologically characterized and systematically compared with reference plasmas obtained by macro centrifugation of the considered samples (5min, 1500g, 20°C). Firstly a lysis percentage is estimated with Cripps method [5] and using a linear standard curve obtained by the dilution of a reference lysed sample. Then the proteins amount is rapidly and roughly approximated by Beer's law at 280nm. These absorbance measures are carried out with a UV-visible spectrophotometer (Cary300, Varian). Aspartate aminotransferase (AST) enzyme activity is also monitored with Cholestech LDX System and corresponding ALT-AST test cassettes.

In the mean time, residual cells can be observed off-chip. Red cells are directly counted with a haemocytometer (Quick Read, Globe Scientific INC). Platelets and white cells are selectively stained with (anti-CD61 and anti-CD45 respectively) FITC-labeled antibodies (BD Biosciences).

III. Flows and phenomena

According to Segré and Silberberg [12], neutrally buoyant particles in straight microchannels experience a lateral migration: a lift force due to the wall combined with a drag due to the shear flow. This migration is also observed for

blood cells, due to their deformability sufficient to induce lift forces in Poiseuille flow. An expression of this lift force (F_L) (1) has been experimentally established by Abkarian et al. [13], with η the fluid viscosity, $\dot{\gamma}$ the applied shear rate, R the cell radius, h the distance between the wall and the particle and $f(v)$ a function depending on the cell reduced volume.

$$F_L = \eta\dot{\gamma}\frac{R^3}{h}f(v) \quad (1)$$

Consequently a boundary layer of some microns, called the cell-free layer, becomes depleted of cells, followed by an over-concentrated ring (Figure 1a and 1b) [14]. This cell-free layer makes possible to extract a clear plasma volume, by branching it off into appropriate side channels. This effect has been recently exploited in some devices, named migration devices [10, 11].

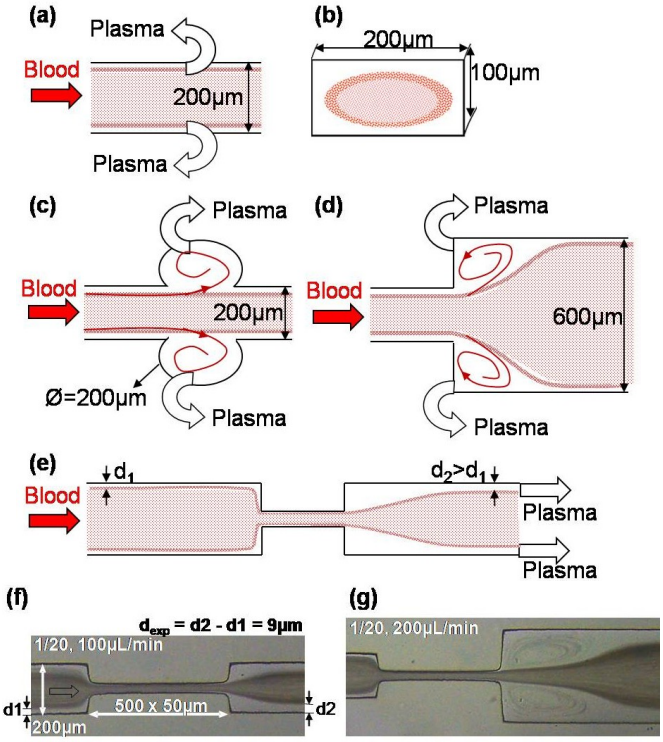

Fig. 1. Phenomena, flows and schematics. (a) Red cells lateral migration and the resulting cell-free layer, which has a circular profile in square section channels (b). (c, d) The cell-free layer feeds geometric singularities to locally increase the clear plasma region. Recirculations in singularities can help to clear this region. (e) A constriction of the channel increases the cell-free layer downstream to facilitate plasma extraction, as in [8, 9]. (f, g) Photographs of 1:20 diluted blood injections showing respectively the restriction effect and the recirculating flows.

Herein the clear plasma region is locally expanded by geometric singularities, such as an abrupt enlargement of the channel (widened from 200 to 600µm) or a cavity along the channel (with a 200µm diameter). As explained in Figure 1c and 1d, these singularities are fed with the plasma coming from this upstream cell-free layer. In this way, the clear region is locally and significantly expanded and the plasma could be then easier extracted. In both singularities, recirculating flows also appear (Figure 1g) and grow with the flow rate, until they occupy the whole extent of singularities at 150µL/min (R_e=11). These recirculations are seen to eject some red cells and repel them in the main flow, due to the centrifugal force applied on red cells and their density higher than plasma. These recirculations have a well-known power of separation, as exploited in [15], dealing with a density-based beads separation in such micro-vortices.

An extra useful phenomenon is the restriction effect. As explained by Faivre et al. in [8], a geometrical constriction of the channel can increase the cell-free layer downstream and make the plasma extraction easier, as proposed in [8, 9] (Figure 1e). So a constriction located upstream of our singularities could additionally expand the plasma and increase extraction yield. This drift d, also called expansion dimension, induced on the cells is defined by (2) [8],

$$d \approx 6\kappa\frac{LR^3}{wh^2} = 0.26 + 0.24\frac{Lw_C}{w^2} \quad (2)$$

where L and w are the length and width of the constriction, w_C the upstream channel width, R the cell radius and κ a dimensionless parameter equal to 0.45. The 9µm expansion measured in Figure 1f is coherent with the 9.86µm expansion calculated by this equation.

IV. Devices for Plasma Extraction

Devices have been designed using these different phenomena for plasma extraction and are characterized in the following chapter.

A. Extraction principle

Blood sample is introduced in inlet (I) channels, whereas plasma is collected in the outermost channels (O_E). Q_I, Q_O and Q_E are the corresponding flow rates, C_I, C_O, and C_E the concentrations (Figure 2a).

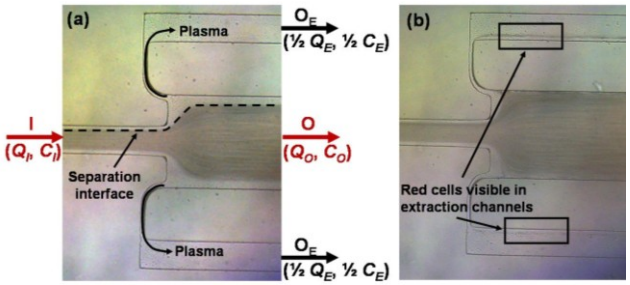

Fig. 2. Enlargement device and experimental principle of plasma extraction, for an injection of 1:20 diluted blood at 100µL/min. (a) Plasma is collected in two lateral extraction channels. The separation interface (dotted line) moves as the plasma extraction is expanded. (b) After a critical Q_E, red cells invade plasma channels (rectangles).

By using a combination of syringe pumps (KdScientific), Q_I and Q_O can be independently controlled. For a given injection flow rate, Q_E is slowly increased as long as a clear extraction is possible. In the mean time, the boundary between the clear plasma and the red cells flow, called the separation interface, is progressively translated towards the

wall. After a critical Q_E, red cells invade and contaminate plasma channels (Figure 2b). This maximal Q_E allowing to get a cell-free plasma defines the extraction yield Q^* (3).

$$Q^* = \frac{Q_E}{Q_I} \quad (3)$$

B. *Extraction yields and optimization*

The maximum extraction yields have been carefully investigated for different geometries and different flow rates, varying from 25 to 175µL/min, following the extraction principle explained before (with Q_O and Q_I independently controlled and Q_E progressively increased). Figure 3 sums up these successive geometrical optimizations.

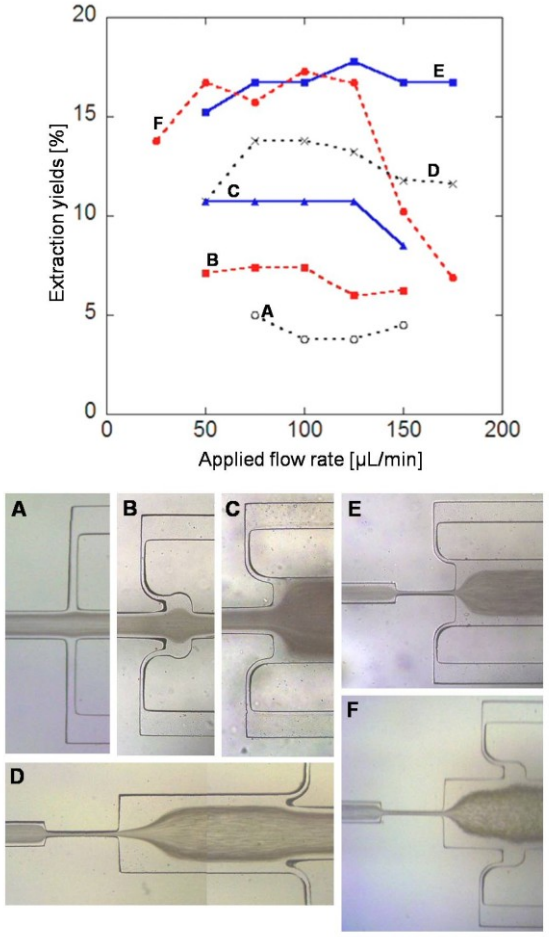

Fig. 3. Extraction yields versus applied flow rates varying from 25 to 175µL/min, for different devices (A, B, C, D, E, F) and for a 1/20 blood injection.

Device A is the basic reference designed to perpendicularly exploit the cell free layer. The devices B and C contain the proposed singularities, respectively the cavity and the enlargement, and provide extraction yields higher than for A device (7.4 and 10.7% versus 5%). This confirms the interest of our geometries that locally expand the clear plasma region before its extraction. Device D introduces the restriction effect and directly extracts the enhanced cell-free layer for a maximal yield of 13.8%. Finally devices E and F present a combination of all these phenomena. The initial cell-free layer is firstly enhanced by a channel constriction before its use by singularities. The scored extraction yields are 17.3 and 17.8%, which confirms again the interest of singularities (regarding the 13.8% of device D) but also the optimization due to restriction effect (regarding the 7.4 and 10.7% of devices B and C).

This graph also defines the working range of injection flow rates which are well appropriate for our plasma extraction. With a maximal extraction rate and a fast stabilization of the fluidic set-up, 100µL/min seems an appropriate working flow rate for further experiments.

C. *Where are the cells?*

The next step is the estimation of extraction purity. This can be defined by red cells contamination ratio (C^*) given by concentration in extracted plasma (C_E) relative to the initial concentration of injected sample (C_I) (4):

$$C^* = \frac{C_E}{C_I} \quad (4)$$

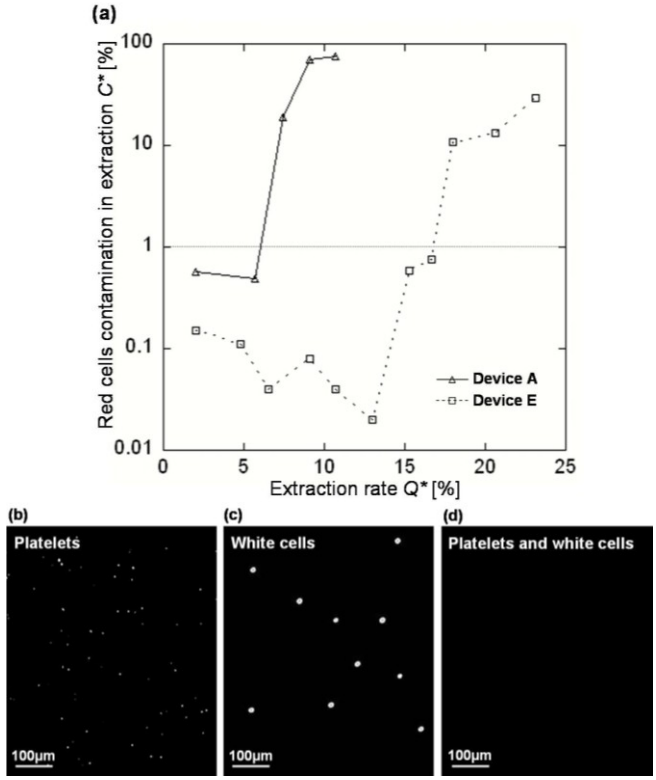

Fig. 4. Plasma extraction from 1:20 blood injected at 100µL/min and cells contamination. (a) Red cells contamination, represented with a logarithmic axis, as a function of extraction yield. 1% (dotted line) is the reference purity scored for plasma extracted by classical centrifugation. (b, c) Stained platelets and white cells of injected sample. (d) Same staining conditions for plasma extracted at Q^*=7.4% with device E.

In Figure 4, C^* is represented as a function of the extraction rate, for 1:20 diluted blood injected at 100µL/min and for 2 devices: device A as a reference design and device E as the optimal design. As observed and explained in Fig.2, C^* remains weak and constant, lower than 1% (which is the

reference purity scored for a plasma extracted by classical centrifugation) until the threshold of 17% extraction yield where C^* suddenly jumps to 10%, corresponding to the red cells invasion in extraction channels. This threshold defines a working range of extraction yields, where plasma purity can be considered as excellent.

Other purity experiments consist in staining platelets and white cells in injected and extracted samples. Figure 4b, c and d illustrate that for Q^*=7.4%, the extracted plasma contains neither platelets nor white cells compared to the injected sample. Therefore proposed devices allow an extraction with excellent cell purity (red cells contamination lower than for classical centrifugation, no platelets and no white cells). This could be useful since specific studies on growth factors such as VEGF (vascular endothelial growth factor) would require platelet-depleted plasma.

Different cellular parameters are involved in this fluidic repartition, such as the cell dimensions and its form (spherical for white cells or ellipsoid for red cells) but also its deformability, making complex the interpretation of these results. Further studies should help the understanding.

D. Plasma characterization

Extracted plasma has been biologically characterized for 5 different donors and compared with reference plasmas obtained by classical centrifugation of the same samples.

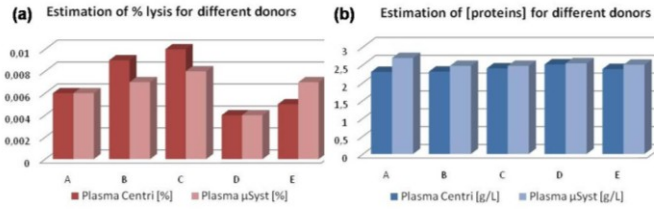

Fig. 6. Characterization of plasma extracted by the device E, from 5 different donors (A, B, C, D, E) and for 1:20 blood injected at 100µL/min, compared with reference centrifuged plasma. (a) Comparison of the lysis percentages estimated with Cripps method. (b) Comparison of the proteins concentrations estimated with Beer's law at 280nm.

Figure 6a represents an estimation of the lysis percentage. It confirms that no hemoglobin seems additionally released in the plasma by red cells and validates that our devices don't generate any notable haemolysis in spite of a strong shear stress. Figure 6b illustrates the determination of the whole proteins amount and shows that no proteins loss in plasma is detectable. The slightly higher protein concentration obtained for extracted plasma does not seem statistically significant. Additional experiments (data not shown) also confirm that plasma aspartate aminotransferase doesn't seem to be denatured by this microfluidic extraction.

V. Conclusion

Herein original and passive geometries have been proposed to continuously carry out plasma extraction. These devices have been characterized and optimized, with extraction yields up to 17.8% from 1:20 diluted blood, giving a 3-fold improvement compared to the basic device. The extracted plasma has also been biologically validated, showing neither haemolysis nor proteins loss. The good purity of our plasma, especially about platelets, can suggest many applications such as growth factors studies.

The following steps will firstly consist in estimating the sample dilution effect. Then the extraction yield will be increased, by further designs optimizations and above all by the arrangement of several designs in series or in parallel.

Acknowledgments

The authors are grateful to Manuel Alessio and Regis Blanc for the silicon molds microfabrication.

References

[1] M. Toner, and D. Irimia, "Blood on a chip," *Annu. Rev. Biomed. Eng.*, 2005, **7,** 77-103.
[2] N. Pamme, "Continuous flow separations in microfluidic devices," *Lab on a Chip*, 2007, **7,** 1644-1659.
[3] M. Kersaudy Kerhoas, R. Dhariwal, and M. Desmulliez, "Recent advances in microparticle continuous separation," *IET Nanobiotechnol.*, 2008, **2,** 1, 1-13. July 1993.
[4] E. Sollier, H. Rostaing, Y. Fouillet, J.L. Achard, and P. Pouteau, "Passive microfluidic devices for plasma extraction from whole human blood," *Sensors & Actuators, Chemical,* 2009, in press.
[5] V. VanDeLinder, A Groisman, "Separation of plasma from whole human blood in continuous cross-flow in a molded microfluidic device," *Anal. Chem.*, 2006, **78,** 3765-3771.
[6] H. Ji, V. Samper, Y. Chen, K. Heng, T.M. Lim, and L. Yobas, "Silicon based microfilters for whole blood cell separation," *Biomed. Microdevices*, 2008, **10,** 251-257.
[7] A. Nilsson, P. Petersson, and T. Laurell, "Whole blood plasmapheresis using acoustic separation chip," *Proc µTAS Conference*, 2006, Tokyo, Japan, 1154-1156.
[8] M. Faivre, M. Abkarian, K. Bickraj, and H. Stone, "Geometrical focusing of cells in a microfluidic device: an approach to separate blood plasma," *Biorheology,* 2006, **43,** 147-159.
[9] M. Kersaudy Kerhoas, R. Dhariwal, M. Desmulliez, and L. Jouvet, "Blood flow separation in microfluidic channels," *Proc µFlu'08*, 2008, Bologna, Italia.
[10] R.D. Jäggi, R. Sandoz, and C.S. Effenhauser, "Microfluidic depletion of red blood cells from whole blood in high aspect ratio microchannels," *Microfluid. Nanofluid.,* 2007, **3,** 47-53.
[11] S. Yang, A. Ündar, and J.D. Zahn, "A microfluidic device for continuous real time plasma separation," *Lab on a Chip*, 2006, **6,** 871-880.
[12] G. Segré, and A. Silberberg, "Behaviour of macroscopic rigid spheres in Poiseuille flow: Part 2. Experimental results and interpretation," *J. Fluid. Mech.*, 1962, **14,** 136-57.
[13] M. Abkarian, and A. Viallat, "Dynamics of vesicles in a wall-bounded shear flow," *Biophys. J.*, 2005, **89,** 1055-1066.
[14] G. Thurston, "Plasma release-cell layering theory for blood flow," *Biorheology*, 1989, **26,** 199-214.
[15] D.T. Chiu, "Cellular manipulations in microvortices," *Anal. Bioanal. Chem.*, 2007, **387,** 17-20.